Talanta 85 (2011) 983–990

Contents lists available at ScienceDirect

Talanta

journal homepage: www.elsevier.com/locate/talanta

A magnesium hydroxide preconcentration/matrix reduction method for the analysis of rare earth elements in water samples using laser ablation inductively coupled plasma mass spectrometry

Hui-Fang Hsieh [a], Yi-Hsiang Chen [a], Chu-Fang Wang [a,b,*]

[a] Department of Biomedical Engineering and Environmental Sciences, National Tsing Hua University, Hsinchu 30013, Taiwan
[b] Institute of Nuclear Engineering and Science, National Tsing Hua University, Hsinchu 30013, Taiwan

ARTICLE INFO

Article history:
Received 18 March 2011
Received in revised form 3 May 2011
Accepted 5 May 2011
Available online 12 May 2011

Keywords:
Rare earth element
Magnesium hydroxide
Preconcentration
Laser ablation
Inductively coupled plasma mass spectrometry

ABSTRACT

This paper describes a simple method for simultaneous preconcentration and matrix reduction during the analysis of rare earth elements (REEs) in water samples through laser ablation inductively coupled plasma mass spectrometry (LA–ICP–MS). From a systematic investigation of the co-precipitation of REEs using magnesium hydroxide, we optimized the effects of several parameters – the pH, the amount of magnesium, the shaking time, the efficiency of Ba removal, and the sample matrix – to ensure quantitative recoveries. We employed repetitive laser ablation to remove the dried-droplet samples from the filter medium and introduce them into the ICP–MS system for determinations of REEs. The enrichment factors ranged from 8 to 88. The detection limit, at an enrichment factor of 32, ranged from 0.03 to 0.20 pg mL^{-1}. The relative standard deviations for the determination of REEs at a concentration of 1 ng mL^{-1} when processing 40 mL sample solution were 2.0–4.8%. We applied this method to the satisfactory determination of REEs in lake water and synthetic seawater samples.

1. Introduction

Because rare earth elements (REEs) are often used in modern industrial applications, to take advantage of their metallurgical, optical, and electronic properties, their release into the environment has increased [1,2]. For example, there are many recent reports of anomalous levels of Gd in the REE distribution patterns in coastal seawater, presumably caused by the discharge of Gd compounds used as magnetic resonance imaging contrast reagents. Because of the high stability of such compounds, this Gd anomaly is a possible indicator of anthropogenic impact on aqueous environments [3,4]. For this and other reasons, the determination of accurate levels of REEs is necessary for environmental monitoring and geological studies.

Among the many analytical techniques that have been used for the determination of REEs in aqueous samples, neutron activation analysis [5,6], isotope dilution mass spectrometry [7], inductively coupled plasma atomic emission spectrometry (ICP–AES) [8–12], and inductively coupled plasma mass spectrometry (ICP–MS) [13–22] are the most popular. Nevertheless, the direct determination of REEs in natural water samples remains a challenge because their concentrations are generally close to (or lower than) the detection limit of ICP–MS [7,19,20,23] and because the concentration of Ba is typically much higher than those of other REEs, resulting in significant polyatomic interference when measuring La, Sm, Gd, and Eu (e.g., ^{151}Eu and ^{153}Eu suffer interference by $^{135}Ba^{16}O$ and $^{137}Ba^{16}O$, respectively) [7,19]. Furthermore, the high salt content (*ca.* 3%) in seawater can result in clogging of introduction systems and serious interference with REE measurement [20]. To overcome these problems, co-precipitation [12,22], liquid–liquid extraction [13,14], and solid phase extraction [15–21] techniques have been developed to enrich the REEs and remove salts prior to analysis.

Co-precipitation is a separation/preconcentration technique based on phase separation. Analyte ions are precipitated in this procedure using a combination of a carrier element and a suitable chelating agent [12,22,24]. Metal hydroxides [e.g., Fe(III) and Mg] have been used as inorganic co-precipitants for the preconcentration of trace metal ions from aqueous media. The simplicity, ease of availability, and compatibility of co-precipitation methods with different measurement techniques make them appropriate alternatives to expensive and time-consuming separation/preconcentration procedures. One of the drawbacks of co-precipitation is that the relatively high concentration of the co-precipitate carrier can influence the measurement of trace elements. For example, a large quantity of Mg can lead to severely high

* Corresponding author at: Department of Biomedical Engineering and Environmental Sciences, National Tsing Hua University, Hsinchu 30013, Taiwan.
Tel.: +886 3 571 5131 34222; fax: +886 3 572 7298.
E-mail address: cfwang@mx.nthu.edu.tw (C.-F. Wang).

0039-9140/$ – see front matter © 2011 Elsevier B.V. All rights reserved.
doi:10.1016/j.talanta.2011.05.011

background absorption signals during analysis. The use of $Fe(OH)_3$ leads also to the co-precipitation of large amounts of alkaline earth metals [25,26]. Lanthanum hydroxide precipitate coated onto cellulose fibre technique have been adopted as an alternative method to eliminate potential interfering effects from the carrier [27]. Notably, co-precipitation with a carrier requires an additional separation step, usually cation-exchange chromatography, to remove the carrier prior to ICP–MS determination [24].

Laser ablation (LA) systems, connected to ICP mass spectrometers, can be used to ablate solid samples directly for trace and ultra-trace element determination. This technique has been applied to the determination of geological, environmental, and biological samples [28–30]. The formation of refractory REE–O^+ ions – particularly $^{140}Ce^{16}O^+$, $^{139}La^{16}O^+$, and, to a lesser extent, $^{141}Pr^{16}O^+$, BaO^+, and $BaOH^+$ species – is, however, a significant problem in quantitative REE determinations performed using ICP–MS [31]. The conventional method for introducing a sample into the plasma is nebulization of a solution; in this case, prior to analysis, the sample must be dissolved. One of the advantages of LA over solution nebulization, as a means of sample introduction, is that LA creates dry plasma, which might reduce the amount of introduced oxygen, thereby minimizing the presence of interfering oxide species [32,33].

In this study, we developed a simplified $Mg(OH)_2$ co-precipitation method for the determination of REEs using LA–ICP–MS. This method has the advantage of allowing simultaneous preconcentration and matrix reduction during the analysis of REEs in water samples. Moreover, co-precipitation with the carrier requires no additional separation step to remove the carrier prior to ICP–MS determination. We validated the accuracy of these determinations by analyzing a certified river water reference material. Furthermore, we applied this method to the determination of REEs in lake water and synthetic seawater samples.

2. Experimental

2.1. Instrumentation

A UP-213 laser ablation system (New Wave Research, Fremont, CA) was coupled to an Agilent 7500a ICP–MS system (Agilent Technologies, Santa Clara, CA). The LA device contained a frequency-quintupled Nd:YAG (neodymium–doped yttrium aluminum garnet crystal) laser and provided deep-UV irradiation (λ = 213 nm). The laser was operated using a defocused beam having a spot diameter of 110 μm to maximize the laser beam area and produce a relative large signal. As the laser beam moved across the surface of the sample, very rapid heating occurred, causing the matrix to be volatilized or ablated. Argon was used to transport the ablated material from the ablation chamber to the ICP system. The ions formed in the ICP were extracted in the quadrupole mass spectrometer and separated according to their mass-to-charge rations. The mass spectrometer was set up in time-resolved analysis mode, measuring one point per mass [TRA(1)], and acquiring the masses chosen. Peak areas were used for final quantitation of the analyte concentrations. The LA system was fully computer-controlled and featured a real-time video imaging system capable of viewing reflected and transmitted light (polarized light available). The system could be programmed to ablate continuous lines, spots, or a variety of more complex ablation patterns. The LA–ICP–MS operating parameters are summarized in Table 1. The total acquisition time per sample was 230 s, including a 20-s equilibration and stabilization time between each sample droplet ablation event. Optimization of the plasma, and mass spectrometric conditions, was accomplished using solution nebulization prior to switching to LA sample introduction. A mixed-element (Li, Y, Ce, Tl) standard solution (1 ng mL^{-1}) was used to obtain the highest signal-to-background ratio for ^7Li, ^{89}Y, and ^{205}Tl. The doubly charged ratio ($^{140}Ce^{2+}/^{140}Ce^+$) and oxide ratio ($^{156}CeO^+/^{140}Ce^+$) were maintained below 3%, respectively.

Table 1
LA–ICP–MS operating conditions.

Instrument	Parameter	Value
ICP–MS	RF power	1.5 kW
	Plasma argon gas flow	15 L min^{-1}
	Auxiliary argon gas flow	1.0 L min^{-1}
	Make up argon gas flow	0.15 L min^{-1}
	Carrier argon gas	1.0 L min^{-1}
	Sampler/skimmer cone	Nickel
	Acquisition mode	Time-resolved analysis
	Acquisition time	230 s
Laser ablation	Wavelength	213 nm
	Output energy	100%
	Laser energy	17 J cm^{-2} (1.6 mJ)
	Defocus setting	2 mm
	Carrier argon gas	1.0 L min^{-1}
	Laser scanning mode	Grid of spots
	Repetition rate	20 Hz
	Dwell time	8 s
	Intersite pause	5
	Spot size	110 μm
	Raster spacing	200 μm
	Grid spacing	200 μm

Values of pH were measured using a Mettler Toledo MP-220 pH meter (Mettler Toledo, Schwerzenbach, Switzerland) featuring a glass electrode. PTFE filter membranes (Pall Corporation, Ann Arbor, MI) were used as substrates upon which all of the sample aliquots were deposited and dried.

2.2. Reagents and solutions

All chemicals were of analytical grade and used without further purification, except for HNO_3 (65%, v/v; Darmstadt, Germany), which was of Suprapur grade. The deionized water (DIW) used in each experiment and in each cleaning step was obtained through a process of reversed osmosis of tap water, ion exchange, and filtration (Millipore, Molsheim, France).

All calibration solutions were prepared afresh daily from 10 μg mL^{-1} stock solutions (Ultra Scientific, North Kingstown, RI) diluted with 6 N HNO_3. Matrix-matched standards were used for collection of the response curve by spiking $Mg(NO_3)_2$ solution to 8 mM. A certified reference material (CRM) was used to validate the accuracy of the proposed method. The SLRS-4 river water reference material for trace metal analysis was obtained from the National Research Council of Canada (Ottawa, Ontario, Canada).

The lake water sample was collected from Cheng-Kung Lake, Hsinchu, Taiwan. Immediately after sampling, the lake water was filtered through 0.45-μm membrane filter, acidified to approximately pH 2.0 by adding ultrapure concentrated HNO_3, and stored in acid-precleaned polyethylene (PE) bottles. Synthetic seawater was prepared having a composition of 22.0 g L^{-1} NaCl, 4.0 g L^{-1} Na_2SO_4, 0.8 g L^{-1} KCl, 1.6 g L^{-1} $CaCl_2{\cdot}2H_2O$, and 10.7 g L^{-1} $MgCl_2{\cdot}6H_2O$, according to the specifications of Lide [34].

2.3. Co-precipitation procedure

The co-precipitation method was tested with model solutions prior to its application to the lake water and synthetic seawater samples. A 40 mL aliquot of the sample was transferred into a centrifuge tube and then an appropriate amount of a magnesium (Mg) solution was added. A certain amount of 1 N NaOH solution was added to adjust the pH; REEs were co-precipitated with the formed precipitate. The tube was shaken for 5 min and then the solution

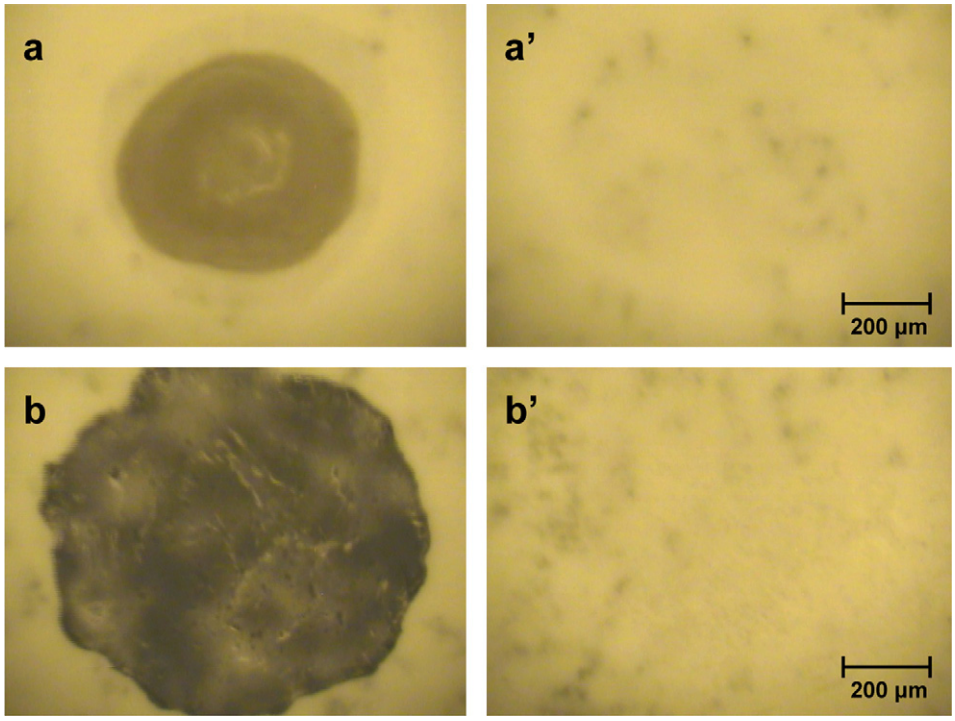

Fig. 1. Still video images of the LA of dried droplets (1 μL) on the PTFE filter membrane. (a) 5 ng mL^{-1} standard solution and (b) lake water with 5 ng mL^{-1} REEs. (a and b) Before and (a′ and b′) after ablation.

was centrifuged (6000 rpm, 10 min). The supernatant was decanted and the remaining precipitate adhered to the tube was dissolved in 6 N HNO_3 (5 mL) for LA–ICP–MS analysis.

2.4. Multi-step $Mg(OH)_2$ co-precipitation procedure

To increase the enrichment factor (EF) when using the proposed method, a procedure was initially tested in which multiple replicates of 40-mL water samples were repeatedly precipitated in a single centrifuge tube. After the Mg precipitate from the previous 40-mL sample had been separated from the supernatant and dissolved in 6 N HNO_3 (400 μL), the solution was mixed with a new replicate of the same sample and then $Mg(OH)_2$ was precipitated upon addition of NaOH. The procedure could be repeated to achieve high enrichment ratios.

2.5. Sample introduction through LA

For LA–ICP–MS analysis, 5 mL of each of the calibration standards and aliquots of the real samples were accurately pipetted into

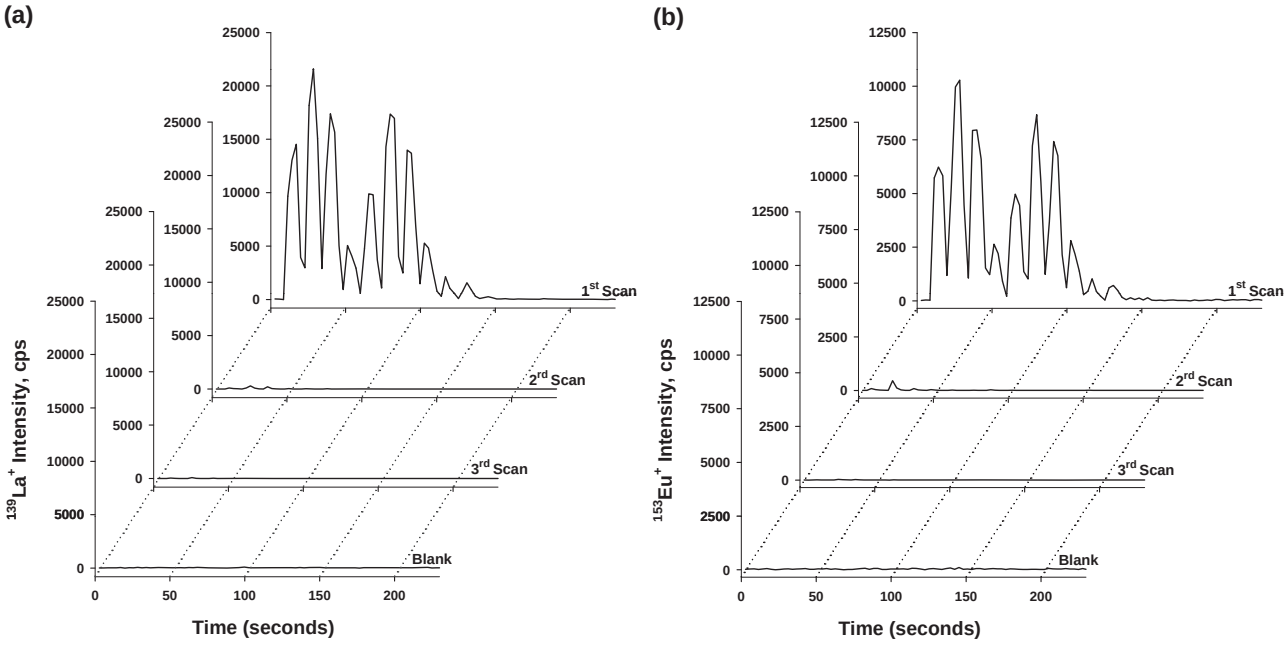

Fig. 2. Responses from (a) $^{139}La^+$ and (b) $^{153}Eu^+$ obtained using LA–ICP–MS. Droplet volume: 1 μL; concentrations of La and Eu: 10 ng mL^{-1} each.

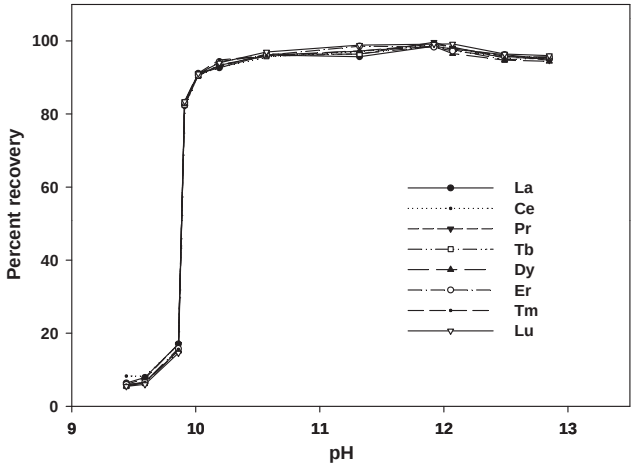

Fig. 3. Effect of pH on the co-precipitation efficiencies of REEs ions ($N = 3$). Shaking time: 5 min; Mg content: 8 mM; concentrations of REEs: 5 ng mL^{-1}.

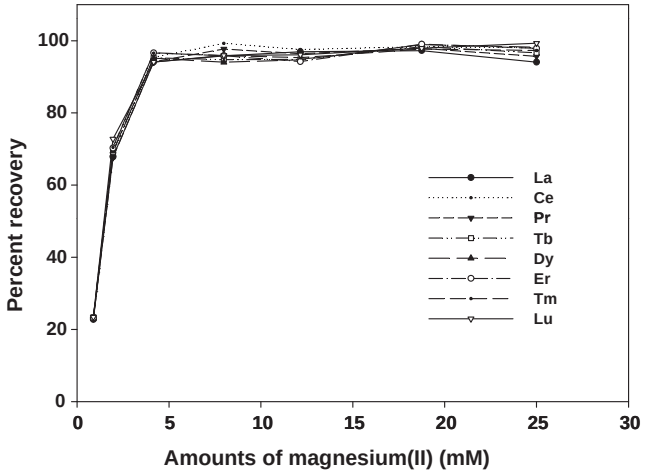

Fig. 4. Effect of Mg content on the co-precipitation efficiencies of REE ions ($N = 3$). Shaking time: 5 min; pH: 10.5; concentrations of REEs: 5 ng mL^{-1}.

10-mL PE tubes. Rhodium standard stock solution (1000 mg L^{-1}, Merck, Darmstadt, Germany) was diluted and added as an internal standard having a concentration of 20 ng mL^{-1}. Methylene Blue was added to 100 μg mL^{-1} as an indicator and to improve the ablation yield. Using a micropipette, 1 μL of each solution was placed onto the surface of a hydrophobic filter membrane, which was then placed under an IR lamp for drying. Because water is repelled from hydrophobic surfaces, the aqueous solutions formed droplets to minimize the contact area; after drying, the residue was present on the surface of the filter membrane in the form of small spots. The dried filter membranes were placed into the LA sampling chamber for further analysis.

3. Results and discussion

3.1. Feasibility of LA–ICP–MS

To generate quantitative data, it is essential that the energy of the laser beam is sufficient to completely remove aerosols from the filter. Fig. 1 presents video images of dried droplets (1 μL) of synthetic seawater and lake water samples on a filter membrane before and after laser ablation. On the hydrophobic substrates, the droplets shrank to leave a spot-like residue much smaller than the initial diameter of the droplet. Depending on the matrix of the sample solution, the diameters ranged from 480 to 850 μm. The diameters of the dried residues derived from the calibrations solutions ranged in size from 480 to 520 μm; those derived from the synthetic seawater had similar diameters. The residues derived from lake water samples exhibited irregular shapes, with diameters of approximately 800–850 μm. The significant discrepancy in spot size between the typical dried standard solutions and lake water samples presumably arose from their different matrix compositions, especially the presence of unidentified organic components, which might have altered the surface tension, in the lake water. Because the sizes of the sample deposits exceeded the diameter of the laser spot, we applied a 4×4 spot grid scanning pattern to ablate the entire sample area. Optimization of the instrument parameters ensured comprehensive sample ablation while maintaining the integrality of the filter membrane during the ablation process. Fig. 1a′ and b′ reveals that no residue remained on the filter membrane, which remained intact, after the ablation process.

Fig. 2 presents the repetitive transit signals of La and Eu (from 10 ng mL^{-1} samples), respectively, providing further evidence for complete ablation. The blank line is the ablation signal of the blank filter membrane. We detected no significant background signals for the targeted analytes during ablation of the filter membrane itself, confirming that no significant contamination occurred from the substrate. Repetitive ablation on the same droplet area revealed that, after initial ablation with appropriate fluence (*ca.* 20 J cm^{-2}), the signal intensities (counts/s) dropped to insignificant levels for all of the measured elements. Thus, complete removal of the ana-

Table 2
Analytical figures of merit.

Element	m/z	R^a	Recovery[b] (%)	MDL[c,d] (pg mL^{-1})
La	139	0.99995	100.9 ± 3.2	0.03
Ce	140	0.99996	101.1 ± 3.6	0.03
Pr	141	0.99997	100.7 ± 4.0	0.03
Nd	143	0.99999	99.4 ± 2.5	0.13
Sm	147	0.99988	100.3 ± 2.7	0.11
Eu	153	0.99994	100.8 ± 3.1	0.06
Gd	157	0.99991	97.5 ± 2.0	0.20
Tb	159	0.99992	99.9 ± 4.0	0.03
Dy	163	0.99998	100.9 ± 3.9	0.11
Ho	165	0.99998	99.9 ± 3.6	0.04
Er	166	0.99998	99.0 ± 3.6	0.06
Tm	169	0.99997	98.9 ± 4.2	0.05
Yb	173	0.99995	97.2 ± 4.8	0.16
Lu	175	0.99995	100.3 ± 4.7	0.04

[a] R: correlation coefficient.
[b] Mean ± standard deviation; N=3.
[c] MDL: method detection limit.
[d] Enrichment factor: 32.

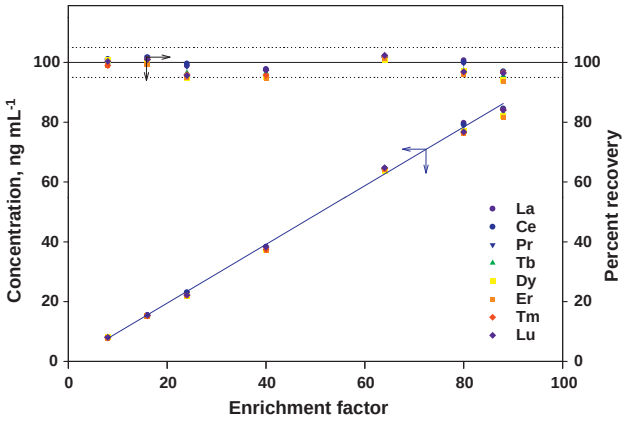

Fig. 5. Efficiencies of multiple replicates of the Mg co-precipitation process. Shaking time: 5 min; Mg content: 8 mM; pH: 10.5; concentrations of REEs: 1 ng mL^{-1}.

lytes from the filter medium had been achieved; in other words, the dried sample droplet was completely ablated during the first scan.

3.2. Optimization of co-precipitation parameters

We investigated the effects of several variables to optimize the accuracy and precision of the preconcentration method. To optimize the co-precipitation conditions for quantitative recoveries, we used DIW spiked with REEs as a model solution and examined the effects of the pH, the amount of Mg, the shaking time, the efficiency of Ba removal, and the sample matrix.

3.2.1. Effect of pH

The pH plays a unique role with respect to the co-precipitation of REEs. Hence, we investigated the influence of the pH on the recoveries in the pH range from 9.4 to 13 using 40 mL of a model solution containing 5 ng mL^{-1} of each REEs. Fig. 3 reveals that the co-precipitation efficiency for all investigating elements was poor when the solution pH was less than 10. On the other hand, the co-precipitation efficiency for all elements reached nearly 100% when the solution pH was equal to 10. Literature reports suggest that alkaline earth metals hydrolyze significantly only at high pH (pH > 9–10) [35]. To separate the REEs from substrates, we selected a pH of 10.5 for all of our subsequent experiments. Furthermore, the experiment should be undertaken when the pH of water sample solution was less than 10.

3.2.2. Effect of the amount of Mg as the carrier element

We examined the effect of the Mg concentration on the co-precipitation efficiencies of the REEs in the range 0.89–33.5 mM. Fig. 4 presents the recoveries of the analytes plotted with respect to the amount of Mg when the reaction was performed at pH 10.5. The recoveries of all elements increased notably upon increasing the amount of Mg; the maximum recoveries were obtained when the Mg concentration was greater than 4.2 mM. Therefore, we chose a Mg concentration of 8 mM for all of our subsequent co-precipitation experiments.

3.2.3. Effect of shaking time

To ensure that equilibrium was established in the REE co-precipitation process, we investigated the influence of the shaking time on the recoveries. A subsidiary experiment revealed that we achieved recoveries of greater than 96% for all of the analytes when the shaking time was 5 min.

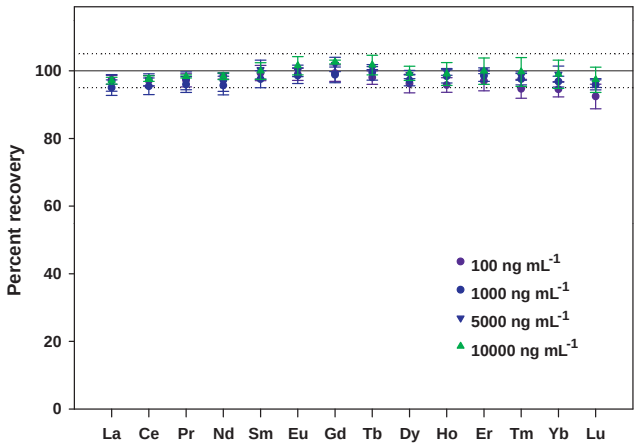

Fig. 6. Analyses of REEs ions at various concentrations of Ba. Shaking time: 5 min; Mg content: 8 mM; pH: 10.5; concentrations of REEs: 1 ng mL^{-1}.

3.2.4. Repeated co-precipitation

Repeating the proposed procedure provided high EFs. We varied the multiple-step $Mg(OH)_2$ precipitation process from 1 (EF = 8) to 11 (EF = 88) replicates using 40 mL model solutions containing 1 ng mL^{-1} of each REE. Using this procedure, the amount of Mg from each precipitation step was reproducible; the recovery of each spiked REE did not decrease upon increasing the number of precipitation steps (Fig. 5).

3.2.5. Effect of Ba^{2+} interference

Separation of Ba is critical in REE analysis because the oxides of the five most abundant Ba isotopes have masses overlapping with those of Sm, Eu, and Gd. Barium is highly enriched in natural water samples relative to the levels of REEs [7,19]. Isobaric interference of Ba and BaO ions with La, Eu, Yb, and Lu ions has also been reported [36,37]. The low first ionization potential of Ba (5.12 eV) reduces the ionization efficiency of the REEs, thereby degrading the quality of the data [36].

We investigated the influence of Ba at concentrations in the range 100–10,000 ng mL^{-1} on the recoveries of REEs in model solutions containing 1 ng mL^{-1} REEs. Fig. 6 reveals that the percentage

Table 3
Analytical results of REEs in SLRS4.

Element	Present work (pg mL^{-1})[a]	Reported [37] (pg mL^{-1})	$\lvert\bar{x}_2 - \bar{x}_1\rvert$[b]	$t\,S_D$[c]
La	281.7 ± 9.4	287 ± 8	5.3	9.2
Ce	354.2 ± 12.1	360 ± 12	5.8	13.7
Pr	70.1 ± 3.1	69.3 ± 1.8	0.8	2.1
Nd	266.3 ± 10.9	269 ± 14	2.7	15.9
Sm	56.3 ± 2.6	57.4 ± 2.8	1.1	3.2
Eu	7.9 ± 0.9	8.0 ± 0.6	0.1	0.7
Gd	33.3 ± 1.6	34.2 ± 2.0	0.9	2.3
Tb	4.6 ± 0.3	4.3 ± 0.4	0.3	0.5
Dy	23.5 ± 0.6	24.2 ± 1.6	0.7	1.8
Ho	4.7 ± 0.4	4.7 ± 0.3	0.0	0.3
Er	13.3 ± 0.9	13.4 ± 0.6	0.1	0.7
Tm	1.8 ± 0.3	1.7 ± 0.2	0.1	0.2
Yb	11.7 ± 0.6	12.0 ± 0.4	0.3	0.5
Lu	1.9 ± 0.1	1.9 ± 0.1	0.0	0.1

[a] Mean ± standard deviation; $N = 3$; enrichment factor: 32.
[b] Indicates the differences in concentration found between the two results. $\bar{x}_1$: observed value; $\bar{x}_2$: reported value.
[c] If the difference between observed and reported value ($\lvert\bar{x}_2 - \bar{x}_1\rvert$) is smaller than the computed value ($t\,S_D$), no significant difference between observed and reported results has been accepted at the 95% confidence level. $S_D = S_{pooled}\sqrt{(N_1 + N_2)/(N_1 \cdot N_2)}$; $S_{pooled} = \sqrt{[s_1^2(N_1 - 1) + s_2^2(N_2 - 1)]/(N_1 + N_2 - 2)}$; t: student's t at 95% confidence; N_1 and N_2, respectively refer to number of replicate measurements in the observed and reported data sets; s_1^2 and s_2^2, respectively refer to variance in the observed and reported data sets.

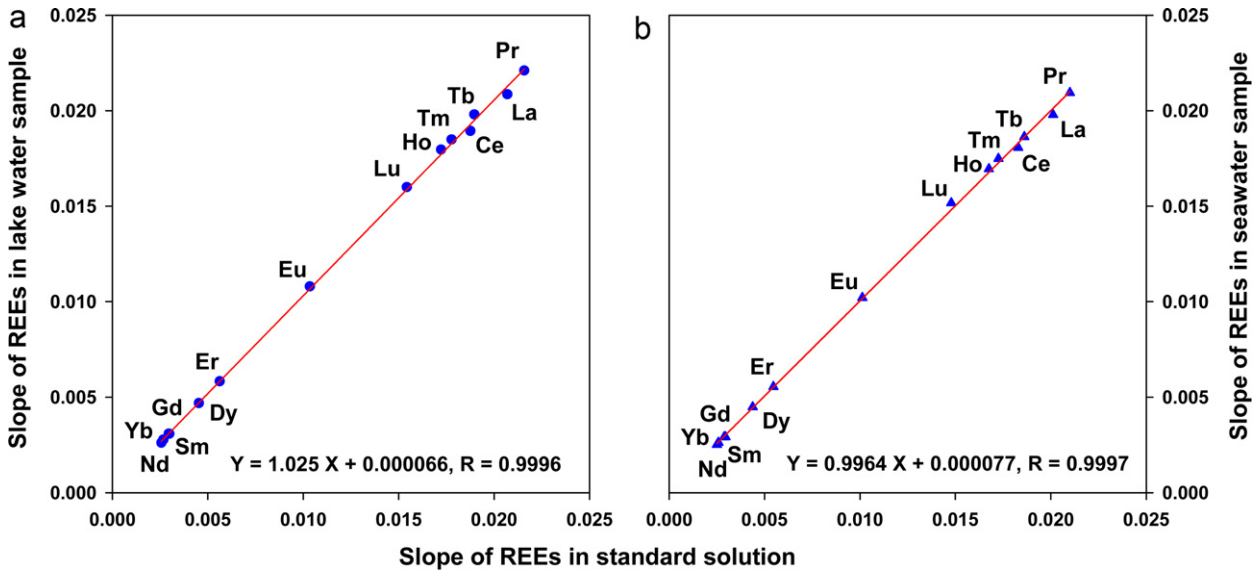

Fig. 7. Slopes of the calibrations for the REEs ions in the (a) lake water and (b) synthetic seawater, plotted with respect to those in the standard samples.

recoveries were quantitative when using the proposed method at each Ba concentration. In other words, Ba and its oxides did not interfere with the determination of any of the REEs. The removal rate of Ba exceeded 99.5% when we co-precipitated the REE model solution at pH 10.5 with 8 mM Mg ions.

3.3. Effect of lake water and synthetic seawater matrices on the determination of REEs

The matrix elements (e.g., Na, K, Mg, Ca) and organic compounds present in water samples often lead to instrument drift, isobaric polyatomic interferences, and signal suppression in the determination of REEs by ICP–MS. We compared the slopes of the calibration curves of the REE ions in the lake water or synthetic seawater samples with respect to those in the standard samples. Fig. 7 reveals that the calibration curves for the REEs ions were in good agreement with one another; the slope ratios for the lake water and synthetic seawater samples were 1.025 and 0.9964, respectively. Therefore, the lake water and synthetic seawater matrices did not interfere with the co-precipitation of REEs ions when using this co-precipitation procedure.

3.4. Analytical figures of merit

Table 2 summarizes the analytical figures of merit, determined using a sample volume, adsorption pH, amount of Mg, and shaking time of 40 mL, pH 10.5, 8 mM, and 5 min, respectively. We examined the analytical performance of the procedure using the results from the LA–ICP–MS measurements. Under the optimized conditions, the calibration curves were linear up to 100 ng mL^{-1} for the studied REEs, with correlation coefficients in the range 0.99988–0.99999. We evaluated the precision of the method in terms of the relative standard deviations (RSDs) of the determinations of REEs (1 ng mL^{-1} of REEs in 40-mL aqueous solution), with the procedure repeated three times under the optimal conditions. The RSDs and the recoveries of the REEs were 2.0–4.8 and 97–101%, respectively. The method detection limits (MDLs) of this method – based on a 3σ criterion, where σ is the estimated standard deviation of seven repetitive measurements of a procedural blank – ranged between 0.03 and 0.20 pg mL^{-1}.

We used SLRS-4, a river water standard reference material for trace metals, to evaluate the accuracy of the proposed method. Because there are no certified values for the REEs, we compared the results obtained from this study with those of Ref. [38]. Table 3 reveals that the observed values were consistent with the reported values, with the student *t*-test indicating that there was no significant difference between the observed and reported values. It is confirmed that this method is applicable to both the preconcentration and determination of REEs through LA–ICP–MS.

3.5. Analytical application

To test whether our developed procedure was valid for real sample analysis using LA–ICP–MS, we studied the recoveries of analytes spiked into real lake water and synthetic seawater samples. Table 4 presents the results from analyses of three replicate samples subjected to preconcentration. The multi-step $Mg(OH)_2$ co-precipitation procedure was performed with four replicates of 40-mL samples repeatedly precipitated in a single centrifuge tube. The results obtained using an EF of 32 indicated that the recoveries were acceptable for trace analysis: 93–98% in the lake water sample and 93–103% in the synthetic seawater sample. That is, quantitative recoveries could be achieved for both types of water samples.

3.6. Comparison with other techniques

Table 5 compares the data from the present method with those of recently reported methods for REE determination. Our proposed method provides data that are comparable – in terms of detection limit and accuracy – with those of other analysis techniques. Compared with other techniques of the co-precipitation of elements using magnesium hydroxide, the sensitivities of our proposed procedure are significantly superior to those obtained by graphite furnace atomic absorption spectrometry [39,40] and differential pulse anodic stripping voltammetry [41]. The advantages of co-precipitation are its relatively simple operation procedure, cost-effectiveness, and applicability to batch processing. The process requires neither careful pH adjustment (indispensable in solid phase extraction) nor any harmful or hazardous organic solvents (necessary in solvent extraction). One of the drawbacks of co-precipitation, however, is that a relatively high concentration of the co-precipitate carrier may influence the measurement of trace elements. Indeed, co-precipitation with a carrier usually necessitates an additional separation step or on-line elution process to remove

Table 4
Analytical results of REEs in water samples.

Element	Spiked (pg mL^{-1})	Lake water		Synthetic seawater	
		Found (pg mL^{-1})	Recovery (%)	Found (pg mL^{-1})	Recovery (%)
La	–	107.3 ± 9.7		97.9 ± 2.3	
	100	202.9 ± 6.4	96	190.7 ± 3.8	93
Ce	–	233.4 ± 10.6		107.6 ± 0.2	
	100	331.2 ± 12.1	98	201.8 ± 5.4	94
Pr	–	29.9 ± 1.7		22.2 ± 0.5	
	100	126.6 ± 3.4	97	118.9 ± 2.9	97
Nd	–	104.6 ± 5.5		49.4 ± 3.2	
	100	201.4 ± 6.5	97	147.0 ± 9.6	98
Sm	–	24.5 ± 2.6		4.1 ± 0.9	
	100	120.5 ± 5.2	96	98.6 ± 0.5	95
Eu	–	8.5 ± 1.0		2.6 ± 0.1	
	100	106.3 ± 2.4	98	100.9 ± 2.4	99
Gd	–	20.8 ± 1.3		4.0 ± 0.8	
	100	116.9 ± 4.3	96	99.4 ± 3.8	95
Tb	–	10.3 ± 0.1		7.6 ± 0.6	
	100	103.1 ± 2.3	93	109.7 ± 0.5	102
Dy	–	19.8 ± 0.5		1.8 ± 0.3	
	100	113.5 ± 1.2	94	101.8 ± 2.7	100
Ho	–	7.5 ± 0.2		3.9 ± 0.2	
	100	100.7 ± 0.4	93	105.7 ± 0.3	102
Er	–	10.9 ± 1.6		3.1 ± 0.4	
	100	104.4 ± 1.3	94	105.3 ± 0.6	102
Tm	–	4.7 ± 0.6		3.9 ± 0.2	
	100	98.4 ± 2.0	94	106.3 ± 0.9	102
Yb	–	9.3 ± 1.3		n.d.	
	100	104.2 ± 2.9	95	100.2 ± 1.0	100
Lu	–	2.7 ± 0.5		1.8 ± 0.1	
	100	97.9 ± 2.4	95	103.1 ± 0.7	101

All data were average using three replicate measurements.
Enrichment factor: 32; n.d.: not detected.

Table 5
Comparison of the REEs analytical performance for different water analysis techniques.

Methods/sample pretreatments	Sample volume, mLSample type EFLOD, pgmL volume (mL)	Sample type	EF	LOD (pg mL^{-1})	%RSD/ng mL^{-1}
ETV–ICP–MS[c]					
Liquid–liquid extraction [13]	2	Lake water, seawater, tap water	5–6	0.02–0.09	4.1–9.2 (0.2)[a]
Liquid–liquid extraction [14]	3.5	River water	7	0.20–0.91	2.5–9.1 (0.1)[a]
ICP–SFMS[c]					
SPME [15]	50	River water	50	0.003–0.9	
ICP–MS[c]					
SPE [16]	50	Seawater	100	0.006–0.06	<2 (0.1)[a]
SPE [17]	1000	Ground water	100	0.05–0.10	<10
SPE [18]	200	River water	40	50–560	
On-line SPE [19]	10	Lake water		0.013–0.15	
On-line SPE [20]	10	Seawater	9.6	0.005–0.09	<10[b]
On-line SPE [21]	200	Seawater	400	0.00143–0.0127	1.1–5.1 (1)[a]
ICP–AES[c]					
SPE [8]	100	Lake water, synthetic seawater	50	3–57	<6 (10)[a]
On-line SPE [9]	20	River water	83–102	2–250	–
On-line SPE [10]	20	River water	83–120	2–95	<10 (1)[a]
On-line SPE [11]	3	River water, lake water, well water	10	30–350	2.1–6.0 (5)[a]
ICP–MS					
Coprecipitation followed by on-line elution [22]	10	River water	10	0.0006–0.20	<3.3 (0.01)[a]
ICP–AES[c]					
Coprecipitation [12]	2000	Ground water	80	8000	<8.1 (50)[a]
Current method/LA–ICP–MS					
Coprecipitation	160	Synthetic seawater, river water	32	0.03–0.2	2.0–4.8 (1)[a]

[a] Concentration level at which the RSD value was obtained.
[b] For all results.
[c] AES: atomic emission spectrometry; ETV: electrothermal vaporization; SFMS: sector field mass spectrometry; SPME: solid phase microextraction; SPE: solid phase extraction.

or dilute the carrier prior to ICP–MS determination [22,24]. Here, we developed a direct sample introduction method for the determination of REEs in dried droplets using LA–ICP–MS. Moreover, the formation of refractory REE–O^+ is a significant problem when performing quantitative REE determinations through ICP–MS [31]. The use of LA can reduce the amount of introduced oxygen species, thereby minimizing the presence of interfering oxide species relative to that obtained when employing wet plasma.

4. Conclusions

Our proposed method for analyzing REEs in real samples is simple and straightforward. The procedure provides excellent preconcentration efficiency, as well as high concentration factors, for analytes in water samples, ensuring the highly sensitive detection of REE analytes. The time required to complete the co-precipitation and determination process was approximately 25 min. The co-precipitated analyte ions were determined sensitively through LA–ICP–MS without any interference from the carrier element. Moreover, the lake water and synthetic seawater matrices did not interfere with the co-precipitation of REEs ions during these procedures. LA creates a dry plasma that reduces the signal intensities for all H–, O–, and OH-based molecular ions, thereby decreasing analyte hydride formation and molecular/polyatomic interference.

Acknowledgments

This study was supported by the National Science Council, Republic of China, under contract number NSC97-EPA-M007-002. We thank the Instrument Center at National Tsing Hua University, Taiwan, for ICP–MS support.

References

[1] T. Pasinli, A.E. Eroğlu, T. Shahwan, Anal. Chim. Acta 547 (2005) 42–49.
[2] K.J.M. Kramer, W.S. Dorten, H. Van het Groenewoud, E. de Haan, G.N. Kramer, L. Monteiro, H. Muntau, P. Quevauviller, J. Environ. Monit. 1 (1999) 83–89.
[3] P. Möller, P. Dulski, M. Bau, A. Knappe, A. Pekdeger, C. Sommer-von Jarmersted, J. Geochem. Explor. 69 (2000) 409–414.
[4] G. Strauch, M. Möder, R. Wennrich, K. Osenbrück, H.R. Gläser, T. Schladitz, C. Müller, K. Schirmer, F. Reinstorf, M. Schirmer, J. Soil Sediments 8 (2008) 23–33.
[5] J.M. Lo, K.S. Lin, J.C. Wei, J.D. Lee, J. Radioanal. Nucl. Chem. 216 (1997) 121–124.
[6] C.P. Lin, B.T. Hsieh, G. Ting, S.J. Yeh, J. Radioanal. Nucl. Chem. 236 (1998) 165–168.
[7] T.J. Shaw, T. Duncan, B. Schnetger, Anal. Chem. 75 (2003) 3396–3403.
[8] P. Liang, Y. Liu, L. Guo, Spectrochim. Acta Part B 60 (2005) 125–129.
[9] R.K. Katarina, M. Oshima, S. Motomizu, Talanta 79 (2009) 1252–1259.
[10] R.K. Katarina, M. Oshima, S. Motomizu, Talanta 78 (2009) 1043–1050.
[11] C.Z. Huang, Z.C. Jiang, B. Hu, Talanta 73 (2007) 274–281.
[12] V. Umashankar, R. Radhamani, K. Ramadoss, D.S.R. Murty, Talanta 57 (2002) 1029–1038.
[13] J. Yin, B. Hu, M. He, Z.C. Jiang, Anal. Chim. Acta 594 (2007) 61–68.
[14] S.W. Wu, M. He, B. Hu, Z.C. Jiang, Microchim. Acta 159 (2007) 269–275.
[15] D. Rahmi, Y. Takasaki, Y.B. Zhu, H. Kobayashi, S. Konagaya, H. Haraguchi, T. Umemura, Talanta 81 (2010) 1438–1445.
[16] D. Rahmi, Y. Zhu, E. Fujimori, T. Umemura, H. Haraguchi, Talanta 72 (2007) 600–606.
[17] C.H. González, A.J.Q. Cabezas, M.F. Díaz, Talanta 68 (2005) 47–53.
[18] K. Hennebrüder, R. Wennrich, J. Mattusch, H.J. Stark, W. Engewald, Talanta 63 (2004) 309–316.
[19] Y.B. Zhu, A. Itoh, T. Umemura, H. Haraguchi, K. Inagaki, K. Chiba, J. Anal. At. Spectrom. 25 (2010) 1253–1258.
[20] Y.B. Zhu, T. Umemura, H. Haraguchi, K. Inagaki, K. Chiba, Talanta 78 (2009) 891–895.
[21] Q. Fu, L.M. Yang, Q.Q. Wang, Talanta 72 (2007) 1248–1254.
[22] Y.B. Zhu, K. Inagaki, H. Haraguchi, K. Chiba, J. Anal. At. Spectrom. 25 (2010) 364–369.
[23] M.G. Lawrence, A. Greig, K.D. Collerson, B.S. Kamber, Appl. Geochem. 21 (2006) 839–848.
[24] C.L. Chou, J.D. Moffatt, Fresenius J. Anal. Chem. 368 (2000) 59–61.
[25] K. Srogi, Anal. Lett. 41 (2008) 677–724.
[26] M.D. Pereira, M.A.Z. Arruda, Microchim. Acta 141 (2003) 115–131.
[27] M.L. Chen, T.T. Yang, J.H. Wang, Anal. Chim. Acta 631 (2009) 74–79.
[28] R.E. Russo, X.L. Mao, H.C. Liu, J. Gonzalez, S.S. Mao, Talanta 57 (2002) 425–451.
[29] S.F. Durrant, N.I. Ward, J. Anal. At. Spectrom. 20 (2005) 821–829.
[30] N.S. Mokgalaka, J.L. Gardea-Torresdey, Appl. Spectrosc. Rev. 41 (2006) 131–150.
[31] C.H. Chung, I. Brenner, C.F. You, Spectrochim. Acta Part B 64 (2009) 849–856.
[32] F. Boué-Bigne, B.J. Masters, J.S. Crighton, B.L. Sharp, J. Anal. At. Spectrom. 14 (1999) 1665–1672.
[33] P. Grinberg, L. Yang, Z. Mester, S. Willie, R.E. Sturgeon, J. Anal. At. Spectrom. 21 (2006) 1202–1208.
[34] D.R. Lide, CRC Handbook of Chemistry and Physics, 88th ed., CRC Press, 2008.
[35] V.L. Snoeyink, D. Jenkins, Water Chemistry, Wiley, New York, 1980.
[36] M.J. Greaves, H. Elderfield, G.P. Klinkhammer, Anal. Chim. Acta 218 (1989) 265–280.
[37] P. Möller, P. Dulski, J. Luck, Spectrochim. Acta Part B 47 (1992) 1379–1387.
[38] D. Yeghicheyan, J. Carignan, M. Valladon, M.B. Le Coz, F. Le Cornec, M. Castrec-Rouelle, M. Robert, L. Aquilina, E. Aubry, C. Churlaud, A. Dia, S. Deberdt, B. Dupré, R. Freydier, G. Gruau, O. Hénin, A.M. de Kersabiec, J. Macé, L. Marin, N. Morin, P. Petitjean, E. Serrat, Geostandard Newslett. 25 (2001) 465–474.
[39] M. Tuzen, K.O. Saygi, M. Soylak, Talanta 71 (2007) 424–429.
[40] S. Saracoglu, M. Soylak, L. Elci, Trace Elem. Electrolytes 18 (2001) 129–133.
[41] T. Yabutani, Y. Utsunomiya, Y. Kado, Y. Tani, H. Kishimoto, A. Fukuda, J. Motonaka, Anal. Sci. 22 (2006) 1021–1024.